



Supplementary Materials for

Pan-tumor genomic biomarkers for PD-1 checkpoint blockade–based immunotherapy

Razvan Cristescu*, Robin Mogg, Mark Ayers, Andrew Albright, Erin Murphy,
Jennifer Yearley, Xinwei Sher, Xiao Qiao Liu, Hongchao Lu, Michael Nebozhyn,
Chunsheng Zhang, Jared K. Lunceford, Andrew Joe, Jonathan Cheng, Andrea L. Webber,
Nageatte Ibrahim, Elizabeth R. Plimack, Patrick A. Ott, Tanguy Y. Seiwert,
Antoni Ribas, Terrill K. McClanahan, Joanne E. Tomassini, Andrey Loboda,
David Kaufman

*Corresponding author. Email: razvan_cristescu@merck.com

Published 12 October 2018, *Science* **362**, eaar3593 (2018)
DOI: 10.1126/science.aar3593

This PDF file includes:

Figs. S1 to S6
Tables S1 to S7
References

Correction: Since the original publication, table S2 has been expanded to include the raw NanoString counts for the housekeeping and predictor genes that make up the GEP score, as well as the weighting algorithm used to determine the score (table S2B).

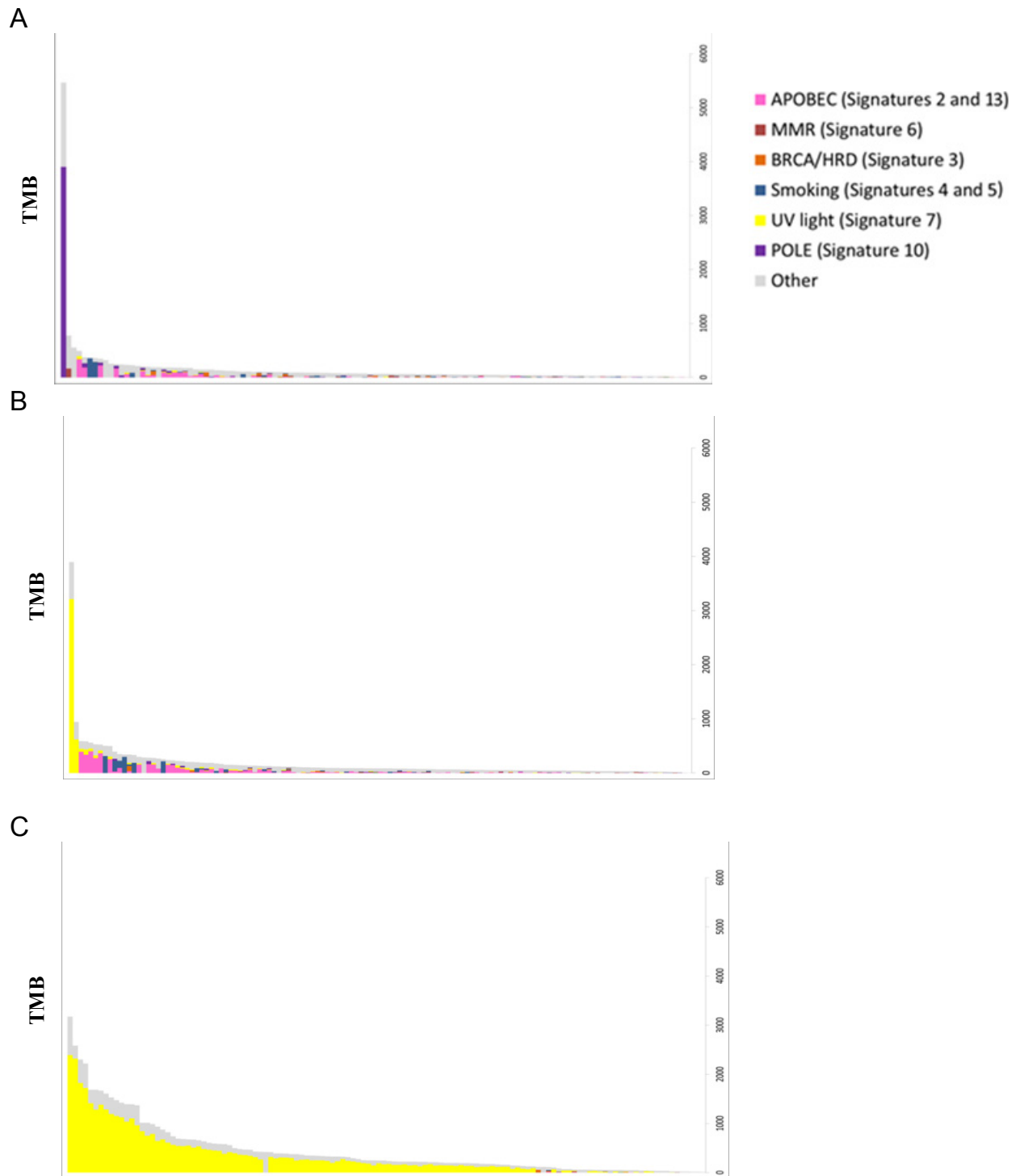


Fig. S1

Distribution and spectrum of TMB across indications. The major signatures(17) displayed above were identified in the mutational landscape of the patients in the clinical cohorts in this study and are illustrated as proportions of the TMB. (A) Pan-cancer cohort, (B) Head and neck, (C) Melanoma.

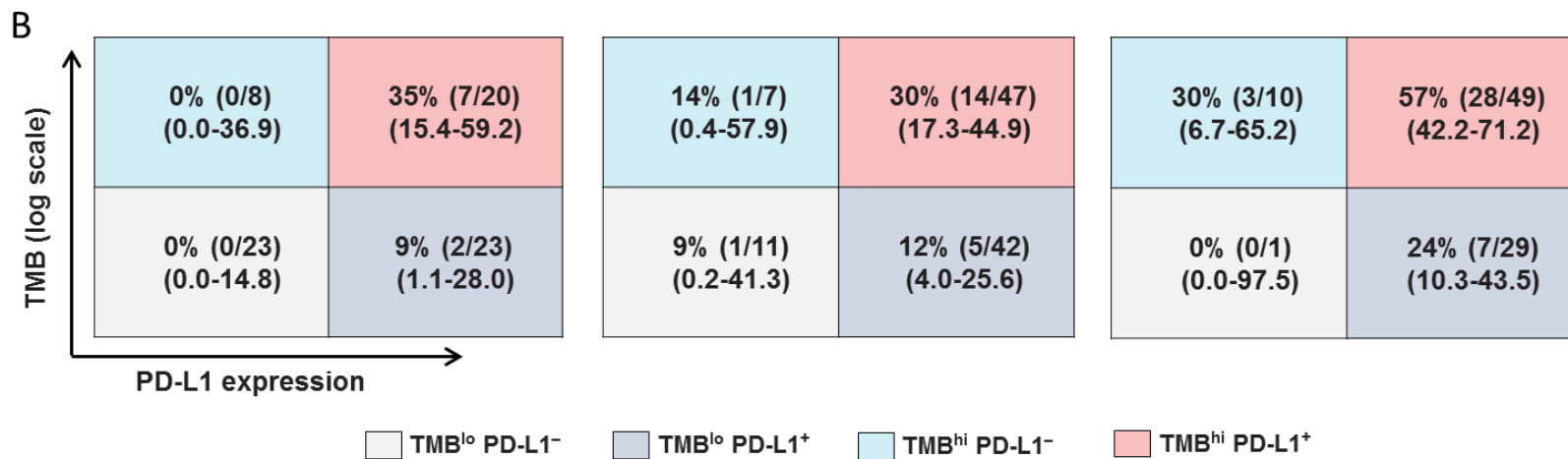
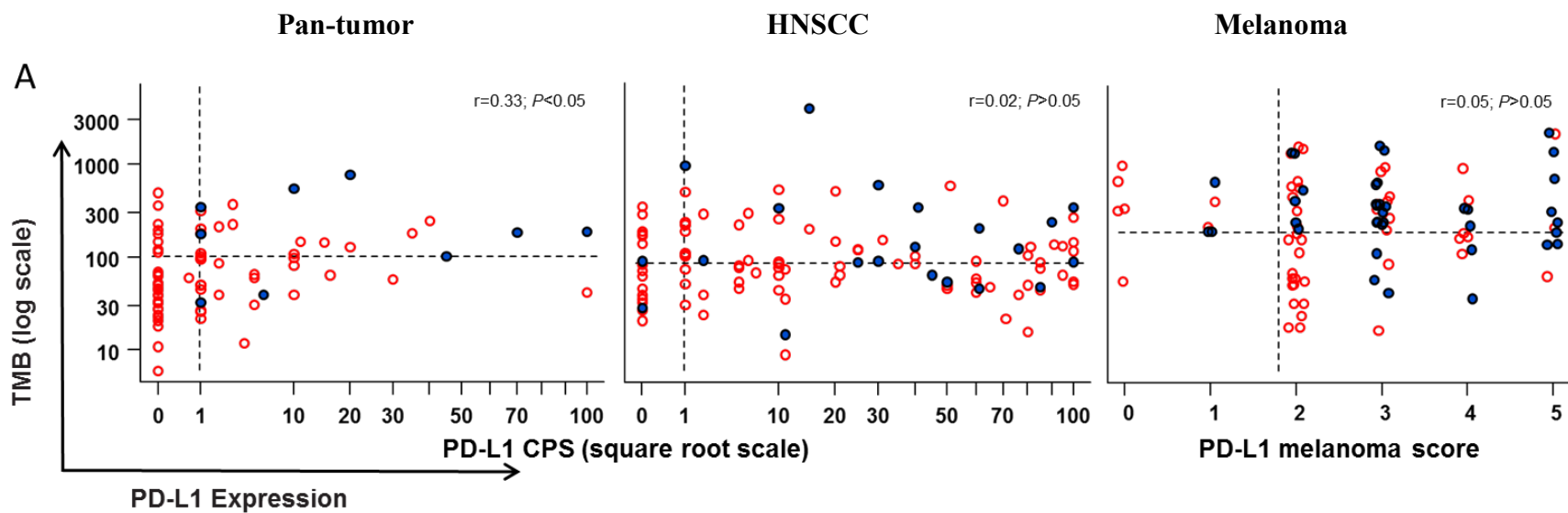


Fig. S2

Relationships between PD-L1 and TMB with BOR in pan-tumor validation, HNSCC and melanoma cohorts. (A) Relationships between TMB and PD-L1 with BOR; responder is PR or CR (filled circles); non-responder is not PR or CR (open circles). Dashed horizontal lines represent the Youden-Index associated cutoffs for TMB in each cohort as derived from AUROCs in Figure 1C. Dashed vertical lines represent PD-L1 CPS cutoff of 1. (B) Response (PR or CR) rates (%; n/N for responder/cut-off defined group, 95% CI) per TMB and PD-L1 cut-off status as designated in (A). TMB^{hi} and PD-L1⁻ response groups are defined by \geq and $<$ Youden-Index associated cutpoints (102.5, 86, 191.5 for pan-cancer, HNSCC, melanoma cohorts, respectively); PD-L1⁺ and PD-L1⁻ groups are defined cut-offs ≥ 1 and 0 respectively.

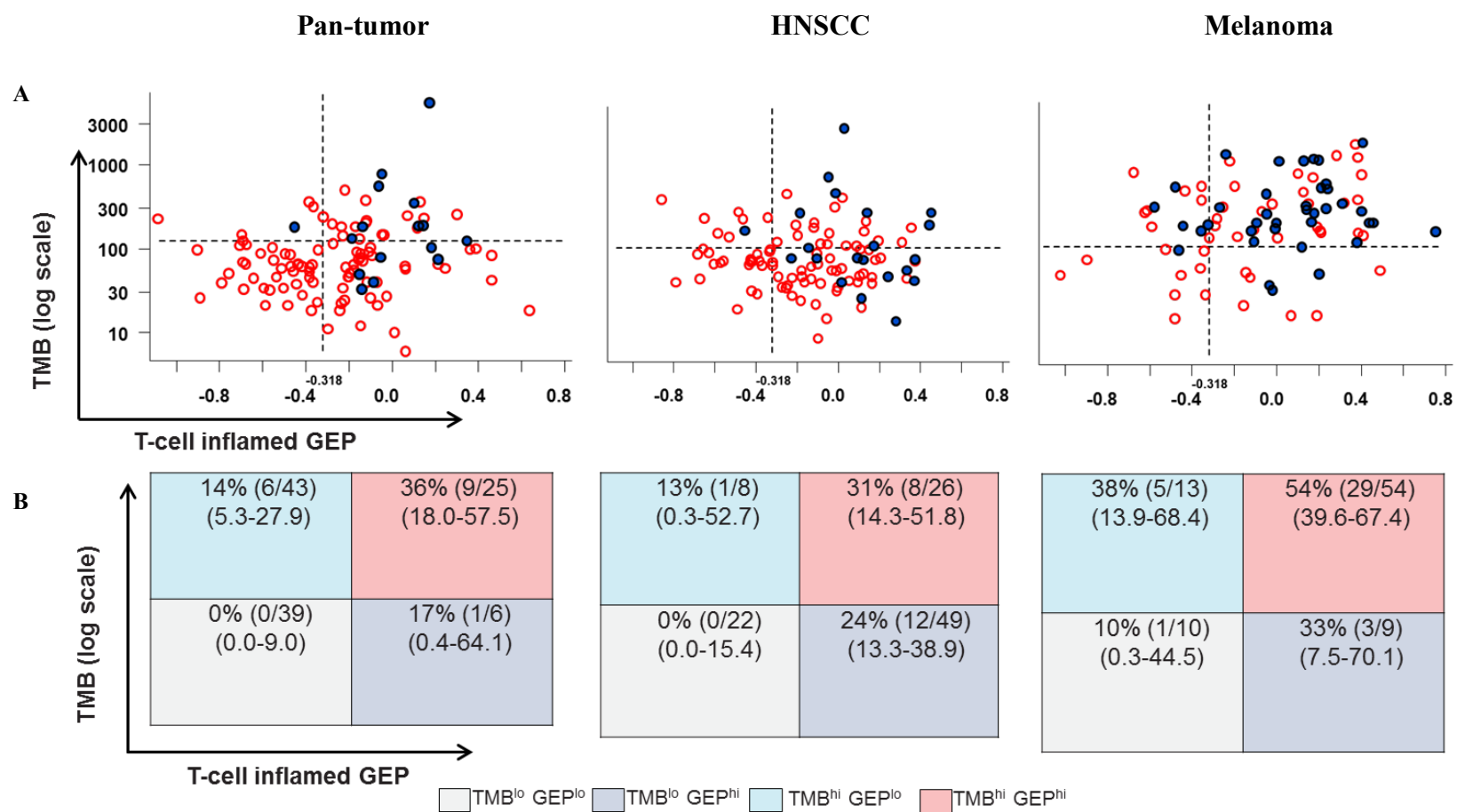


Fig. S3

Relationship between TMB and T cell inflamed GEP with BOR in pan-tumor, HNSCC and Melanoma cohorts at TMB pan-tumor cutoff of 123. (A) Relationships between TMB and T cell-inflamed GEP with BOR; responder is PR or CR (filled circles); non-responder is not PR or CR (open circles). Dashed horizontal lines represent the clinically applicable TMB threshold (TMB ≥ 123

mutations per exome) derived using GEP and TMB data from each cohort (20). Dashed vertical lines represent a discovery cutoff for the T cell-inflamed GEP selected via analysis of pan-cancer data (15). **(B)** Response (PR or CR) rates (% , n/N for responder/cut-off defined group, 95% CI) per TMB and T cell-inflamed GEP cut-off status as designated in (A). For all cohorts, TMB^{hi} and TMB^{lo} response groups are defined by the clinically applicable TMB threshold \geq and $<$ 123, and GEP^{hi} and GEP^{lo} groups are defined cut-offs \geq and $<$ -0.318 respectively. A pan-tumor threshold (20) may be further optimized with additional data beyond those in our study. For example, a pan-tumor TMB threshold of ≥ 175 mutations per exome was recently reported for response to pembrolizumab (21).

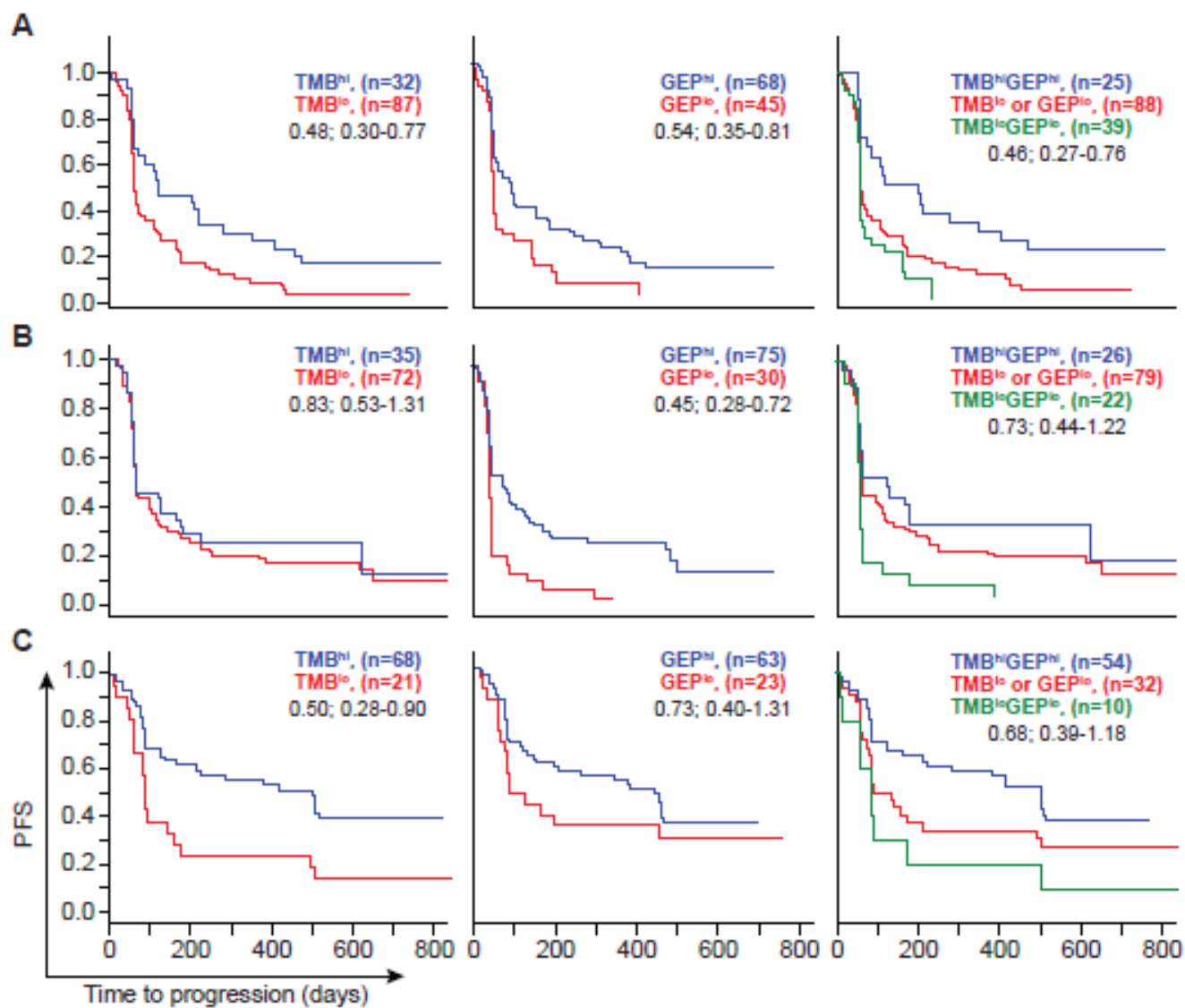


Fig. S4

Relationship between TMB and T-cell-inflamed GEP and PFS in pan-tumor, HNSCC and melanoma cohorts at TMB pan-tumor cutoff of 123. Relationships between TMB and T cell-inflamed GEP with PFS in all patients-as-treated per TMB and GEP cut-offs as described in Fig. S2. Median PFS in days (hazard ratio; 95% CI) for pan-tumor (A), HNSCC (B) and melanoma (C) cohorts respectively for TMB^{hi} vs TMB^{lo} are designated.

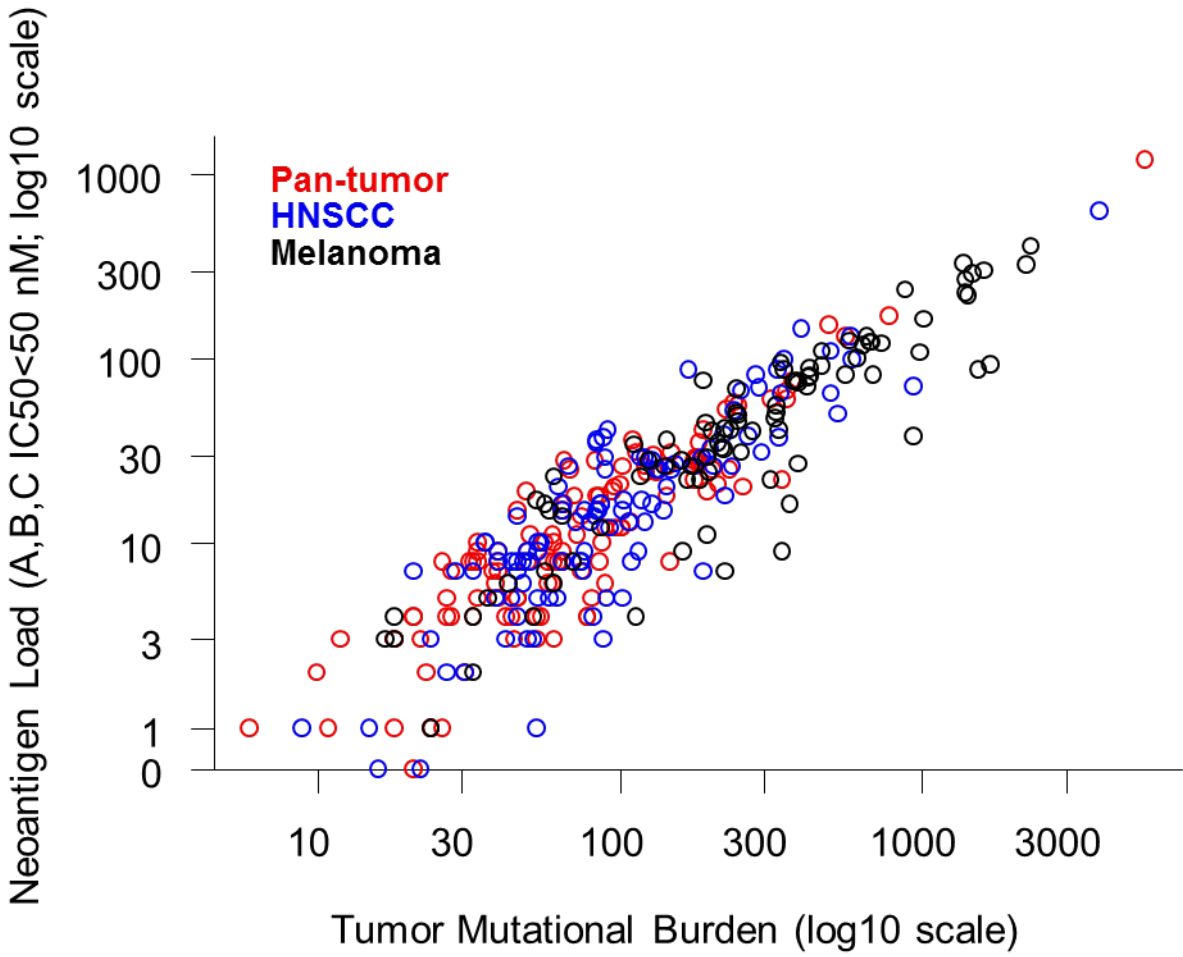


Fig. S5

Relationship between tumor mutational burden (TMB) and neoantigen load. The x and y axes represent TMB and neoantigen load [\log_{10}] respectively and dots represent tumors grouped by the indications used in this study.

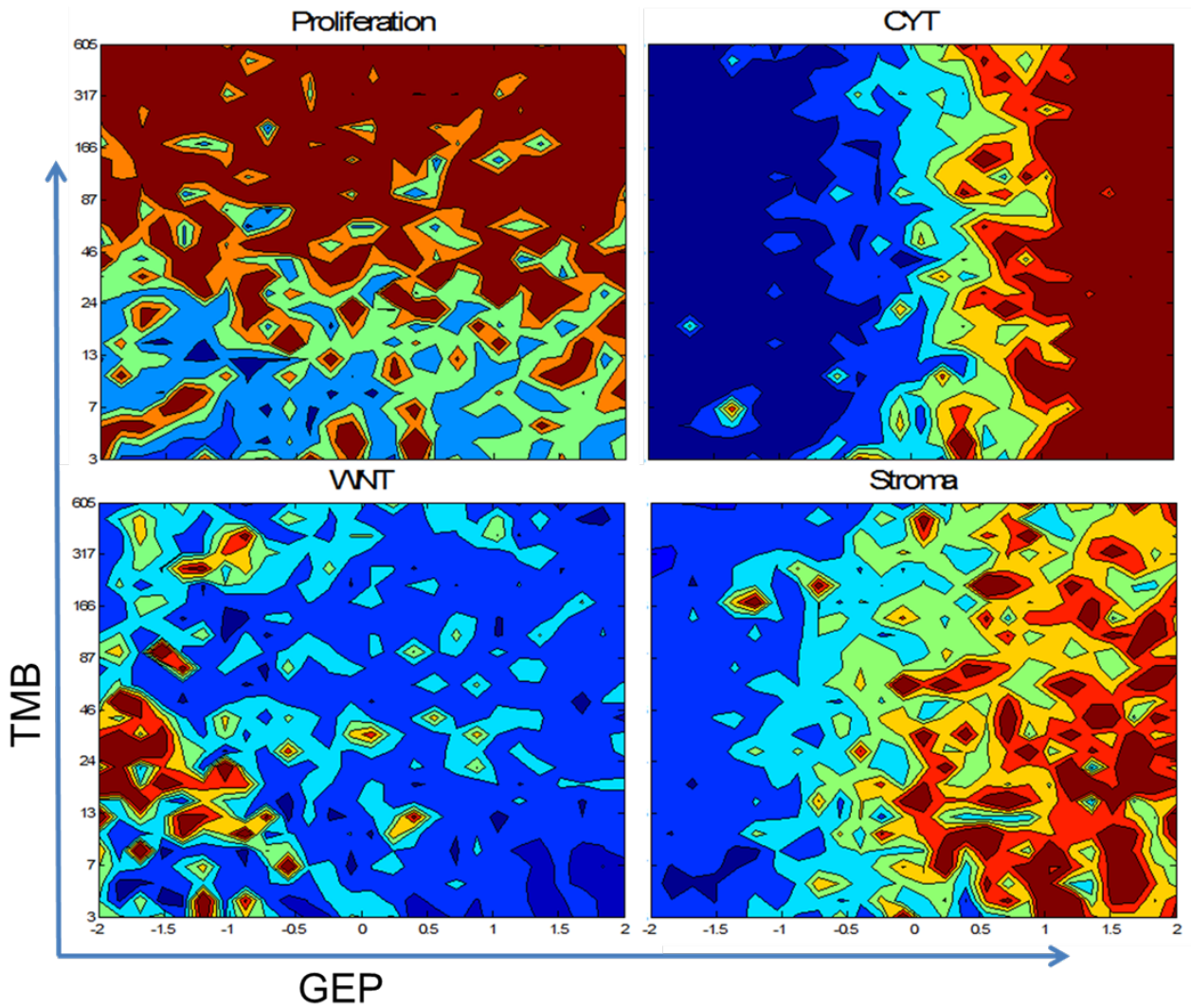


Fig. S6

Association of T-cell-inflamed GEP and TMB with gene signatures in TCGA database.

Contour plots illustrating association of TMB and GEP with selected patterns of biology represented by previously reported gene signatures (13, 31-33) in the TCGA database. Blue/red represent under/over-expression, respectively.

Table S1.
Baseline characteristics of study cohorts

Characteristic n (%)	Pan-tumor KN012/028 N=119	HNSCC KN012 B1/B2 N=107	Melanoma KN001/006 N=89
Age years median (range)	62 (23, 86)	61 (25, 83)	60 (30, 88)
Male	52 (43.7)	88 (82.2)	58 (65.2)
White	77 (64.7)	79 (73.8)	86 (96.6)
Asian	26 (21.8)	17 (15.9)	2 (2.2)
Other	16 (13.4)	11 (10.3)	1 (1.1)
ECOG performance status			
0	41 (34.5)	36 (33.6)	61 (68.5)
1	75 (63.0)	71 (66.4)	28 (31.5)
Unknown	3 (2.5)	0 (0.0)	0 (0.0)
HPV/EBV status			
Positive	17 (14.3)	34 (31.8)	NA
Negative	102 (85.7)	73 (68.2)	NA
<i>BRAF</i> V600			
Wt	NA	NA	69 (77.5)
Mutant	NA	NA	20 (22.5)
ECOG = Eastern Cooperative Oncology Group; EBV = Epstein Barr Virus; HNSCC = head and neck squamous cell carcinoma; HPV = papillomavirus; NA = not applicable			

Table S2.

A. Baseline characteristics of all patients

Patient ID	Age	Sex	Tumor Type	TMB	GEP*	Patient ID	Age	Sex	Tumor Type	TMB	GEP*
001	68	M	Urothelial	180	-0.451	159	56	F	HNSCC Exp	54	-0.291
002	73	M	Urothelial	51	-0.199	160	80	M	HNSCC Exp	204	-0.455
003	72	M	Urothelial	345	0.102	161	55	F	HNSCC Exp	84	0.374
004	67	M	Urothelial	372	-0.122	162	67	M	HNSCC Exp	91	-0.105
005	76	F	Urothelial	40	-0.116	163	61	M	HNSCC Exp	65	-0.179
006	36	F	TNBC	58	0.247	164	76	M	HNSCC Exp	63	-0.010
007	42	F	TNBC	23	-0.347	165	25	M	HNSCC Exp	24	-0.112
008	54	F	Gastric	776	-0.047	166	66	F	HNSCC Exp	55	0.103
009	62	M	Gastric	42	0.459	167	78	M	HNSCC Exp	84	-0.382
010	61	M	Urothelial	86	-0.499	168	67	M	HNSCC Exp	177	-0.198
011	70	F	Urothelial	103	0.181	169	65	M	HNSCC Exp	90	-0.042
012	44	M	Urothelial	66	-0.678	170	67	M	HNSCC Exp	42	-0.246
013	74	M	Urothelial	122	-0.691	171	48	M	HNSCC Exp	44	-0.085
014	76	M	Urothelial	492	-0.221	172	52	M	HNSCC Exp	502	NA
015	70	M	Urothelial	247	0.070	173	53	M	HNSCC Exp	50	-0.131
016	63	F	Urothelial	40	-0.071	174	51	M	HNSCC Exp	584	-0.249
017	78	M	Urothelial	231	0.145	175	49	M	HNSCC Exp	77	-0.101
018	40	F	TNBC	22	-0.234	176	63	M	HNSCC Exp	148	-0.297
019	77	F	Urothelial	65	0.214	177	47	M	HNSCC Exp	3893	0.029
020	49	F	TNBC	44	-0.644	178	54	M	HNSCC Exp	80	-0.573
021	29	F	TNBC	66	-0.437	179	60	M	HNSCC Exp	283	-0.464
022	36	F	TNBC	60	-0.217	180	72	M	HNSCC Exp	526	0.019
023	63	F	TNBC	146	-0.696	181	48	F	HNSCC Exp	46	0.018
024	67	M	Gastric	186	0.124	182	69	M	HNSCC Exp	50	-0.672
025	40	M	Gastric	96	-0.343	183	57	M	HNSCC Exp	36	-0.421
026	65	F	Urothelial	183	-0.234	184	59	F	HNSCC Exp	110	-0.334
027	78	M	Urothelial	100	0.390	185	52	M	HNSCC Exp	118	-0.331
028	60	M	Urothelial	227	-1.087	186	54	M	HNSCC Exp	153	0.196
029	49	F	TNBC	33	-0.687	187	52	M	HNSCC Exp	44	0.166
030	50	F	TNBC	102	-0.556	188	62	M	HNSCC Exp	68	0.017
031	53	F	TNBC	189	0.143	189	55	M	HNSCC Exp	36	-0.009
032	72	F	TNBC	145	-0.039	190	52	M	HNSCC Exp	221	0.356
033	68	F	TNBC	6	0.063	191	67	M	HNSCC Exp	254	-0.118
034	78	M	Gastric	114	-0.275	192	61	F	HNSCC Exp	76	-0.435
035	65	M	Gastric	45	-0.384	193	46	M	HNSCC Exp	59	0.123
036	68	F	Gastric	130	-0.152	194	56	M	HNSCC Exp	89	0.373
037	35	F	Gastric	109	-0.705	195	65	M	HNSCC Exp	92	0.208
038	71	M	Gastric	97	0.360	196	60	F	HNSCC Exp	200	0.126
039	72	M	Gastric	27	NA	197	49	M	HNSCC Exp	22	0.114
040	64	M	Thyroid [†]	50	-0.756	198	59	M	HNSCC Exp	90	-0.229
041	54	F	Carcinoid Tumors	21	-0.589	199	68	M	HNSCC Exp	121	-0.659
042	75	F	Vulvar SCC	57	0.063	200	68	M	HNSCC Exp	21	-0.490
043	54	M	Salivary Gland	32	-0.566	201	64	M	HNSCC Exp	335	-0.185
044	49	F	Anal Canal SCC	143	-0.229	202	59	M	HNSCC Exp	65	0.333
045	55	M	Salivary Gland	12	-0.147	203	63	F	HNSCC Exp	48	0.370
046	56	M	Anal Canal SCC	177	0.116	204	55	F	HNSCC Exp	46	-0.791
047	71	M	Prostate Adeno	123	0.346	205	44	M	HNSCC Exp	54	-0.177
048	47	F	Anal Canal SCC	181	-0.137	206	65	M	HNSCC Exp	119	0.107
049	73	M	Prostate Adeno	65	-0.180	207	60	M	HNSCC Exp	27	-0.183
050	42	F	ER ⁺ HER ⁻ Breast	55	-0.176	208	55	M	HNSCC Exp	188	-0.584
051	65	M	Prostate Adeno	95	-0.903	209	52	M	HNSCC Exp	239	0.441
052	50	F	Leiomyosarcoma	84	-0.472	210	53	F	HNSCC Exp	116	0.151
053	63	F	Anal Canal SCC	195	-0.278	211	64	M	HNSCC Exp	297	-0.345
054	46	F	Anal Canal SCC	46	-0.200	212	60	M	HNSCC Exp	33	-0.393
055	53	F	Salivary Gland	81	-0.093	213	59	M	HNSCC Exp	288	-0.651
056	65	F	Biliary Tract Adeno [‡]	11	-0.297	214	68	F	HNSCC Exp	107	-0.632
057	71	F	SCLC	111	-0.676	215	55	F	HNSCC Exp	53	0.165
058	76	F	Neuroendocrine [§]	60	-0.384	216	62	M	HNSCC Exp	223	-0.120
059	54	F	Colon/Rectal Adeno	73	-0.548	217	61	F	HNSCC Exp	16	-0.057
060	45	M	Colon/Rectal Adeno	86	-0.147	218	54	M	HNSCC Exp	15	0.281
061	72	M	Salivary Gland	61	0.058	219	61	M	HNSCC Exp	499	-0.859
062	70	M	Salivary Gland	69	-0.690	220	73	M	HNSCC Exp	398	-0.016
063	36	F	ER ⁺ HER ⁻ Breast	75	-0.157	221	65	M	HNSCC Exp	190	-0.044
064	54	F	Anal Canal SCC	183	-0.171	222	67	M	HNSCC Exp	87	0.122
065	65	F	Biliary Tract Adeno [‡]	555	-0.061	223	55	M	HNSCC Exp	89	-0.429
066	59	F	Mesothelioma [¶]	24	-0.223	224	50	M	HNSCC Exp	40	-0.003
067	37	F	Cervical SCC	31	NA	225	51	M	HNSCC Exp	340	0.451
068	58	F	Endometrial	53	-0.458	226	71	M	HNSCC Exp	129	0.173
069	69	F	Thyroid Cancer	34	NA	227	54	M	Melanoma	1371	-0.223
070	41	F	Cervical SCC	50	NA	228	68	F	Melanoma	18	0.067
071	43	M	Carcinoid Tumors	28	-1.427	229	62	F	Melanoma	52	NA

Patient ID	Age	Sex	Tumor Type	TMB	GEP*	Patient ID	Age	Sex	Tumor Type	TMB	GEP*
072	72	F	Carcinoid Tumors	21	-0.483	230	70	M	Melanoma	185	0.385
073	66	M	Colon/Rectal Adeno	90	-0.164	231	86	M	Melanoma	114	-0.464
074	55	F	Thyroid†	38	-0.443	232	56	M	Melanoma	677	-0.479
075	73	F	Thyroid†	49	-0.153	233	74	M	Melanoma	57	-1.022
076	23	M	Thyroid†	24	NA	234	76	F	Melanoma	162	0.004
077	53	F	Endometrial	5464	0.174	235	74	M	Melanoma	1607	0.283
078	58	M	Carcinoid Tumors	239	-0.321	236	71	F	Melanoma	418	-0.022
079	43	F	Carcinoid Tumors	63	-0.370	237	61	M	Melanoma	248	0.435
080	65	F	Thyroid†	39	-0.791	238	56	M	Melanoma	2300	0.405
081	74	F	Endometrial	53	-0.381	239	54	F	Melanoma	112	-0.345
082	51	M	Salivary Gland	26	-0.102	240	42	M	Melanoma	53	-0.127
083	57	F	Carcinoid Tumors	18	-0.372	241	63	M	Melanoma	877	0.171
084	48	M	Leiomyosarcoma	58	-0.513	242	30	M	Melanoma	253	0.165
085	71	F	Endometrial	61	-0.418	243	67	F	Melanoma	144	-0.108
086	55	F	Biliary Tract Adeno†	46	-0.205	244	64	M	Melanoma	1015	-0.677
087	59	F	Vulvar SCC	148	-0.046	245	88	F	Melanoma	1392	0.129
088	28	F	Cervical SCC	46	-0.536	246	63	F	Melanoma	65	0.489
089	61	F	Vulvar SCC	27	-0.025	247	66	M	Melanoma	689	-0.200
090	56	M	Mesothelioma [¶]	10	0.011	248	82	M	Melanoma	174	0.411
091	67	F	Mesothelioma [¶]	18	-0.243	249	54	M	Melanoma	225	-0.444
092	68	M	Mesothelioma [¶]	34	-0.502	250	53	M	Melanoma	469	0.384
093	65	M	Mesothelioma [¶]	255	0.299	251	47	F	Melanoma	70	-0.361
094	63	F	Colon/Rectal Adeno	88	-0.611	252	44	F	Melanoma	87	-0.896
095	56	F	Anal Canal SCC	75	0.213	253	66	M	Melanoma	245	0.454
096	56	M	SCLC	358	0.128	254	43	M	Melanoma	1530	0.384
097	86	M	Mesothelioma [¶]	317	-0.366	255	60	M	Melanoma	330	NA
098	63	F	Pancreas Adeno	61	-0.471	256	85	F	Melanoma	18	0.188
099	58	F	SCLC	83	0.460	257	53	F	Melanoma	276	-0.282
100	52	F	Mesothelioma [¶]	40	-0.086	258	34	M	Melanoma	377	-0.270
101	65	M	Esophageal SCC/ Adeno [‡]	132	-0.187	259	57	F	Melanoma	212	-0.009
102	40	F	Esophageal SCC/ Adeno [‡]	90	-0.107	260	76	F	Melanoma	61	NA
103	62	M	Esophageal SCC/ Adeno [‡]	34	-0.596	261	76	M	Melanoma	197	-0.119
104	58	M	Salivary Gland	178	NA	262	55	M	Melanoma	168	-0.187
105	66	M	Salivary Gland	79	-0.055	263	43	M	Melanoma	248	-0.095
106	53	M	Pancreas Adeno	21	-0.069	264	66	M	Melanoma	636	0.240
107	70	M	Biliary Tract Adeno†	33	-0.140	265	77	M	Melanoma	607	-0.434
108	51	M	Biliary Tract Adeno†	102	-0.102	266	39	M	Melanoma	160	-0.318
109	72	M	Salivary Gland	34	-0.229	267	76	M	Melanoma	329	-0.624
110	64	F	Thyroid†	28	-0.415	268	65	M	Melanoma	246	-0.003
111	66	M	Salivary Gland	79	-0.147	269	64	M	Melanoma	43	-0.034
112	65	F	Biliary Tract Adeno†	18	0.637	270	66	M	Melanoma	203	-0.109
113	67	F	Thyroid†	26	-0.891	271	64	M	Melanoma	326	0.175
114	60	M	Thyroid†	65	-0.437	272	59	F	Melanoma	341	-0.072
115	67	F	Colon/Rectal Adeno	71	-0.137	273	65	M	Melanoma	392	0.137
116	47	F	Anal Canal SCC	202	-0.122	274	31	M	Melanoma	190	0.209
117	64	M	Mesothelioma [¶]	213	-0.118	275	43	M	Melanoma	17	-0.483
118	53	M	Mesothelioma [¶]	40	-0.367	276	52	F	Melanoma	385	-0.579
119	53	F	SCLC	358	-0.386	277	68	F	Melanoma	219	0.192
120	50	M	HNSCC	132	0.037	278	57	F	Melanoma	33	-0.481
121	67	M	HNSCC	40	-0.274	279	70	M	Melanoma	1474	0.174
122	63	M	HNSCC	39	-0.251	280	52	M	Melanoma	986	0.100
123	66	M	HNSCC	54	0.242	281	64	F	Melanoma	344	-0.612
124	65	M	HNSCC	62	NA	282	33	M	Melanoma	658	0.210
125	69	M	HNSCC	103	-0.686	283	64	F	Melanoma	364	0.233
126	52	M	HNSCC	237	-0.207	284	62	F	Melanoma	117	-0.525
127	76	M	HNSCC	46	-0.165	285	71	M	Melanoma	142	0.378
128	72	F	HNSCC	144	0.309	286	71	M	Melanoma	225	-0.293
129	64	F	HNSCC	9	-0.097	287	74	M	Melanoma	221	-0.590
130	52	M	HNSCC	87	0.181	288	54	M	Melanoma	389	-0.254
131	83	M	HNSCC	941	-0.046	289	58	F	Melanoma	351	0.140
132	69	M	HNSCC	84	-0.417	290	60	M	Melanoma	126	0.120
133	72	M	HNSCC	82	-0.320	291	49	F	Melanoma	197	-0.358
134	58	M	HNSCC	83	-0.429	292	76	M	Melanoma	465	-0.354
135	70	M	HNSCC	140	-0.088	293	44	M	Melanoma	1423	0.198
136	68	F	HNSCC	85	-0.558	294	73	M	Melanoma	1685	-0.241
137	39	M	HNSCC	29	0.112	295	59	F	Melanoma	683	-0.355
138	72	M	HNSCC	103	-0.393	296	55	F	Melanoma	193	0.751
139	60	M	HNSCC	65	-0.030	297	69	M	Melanoma	428	0.319
140	62	M	HNSCC	170	-0.531	298	81	M	Melanoma	2221	0.372

Patient ID	Age	Sex	Tumor Type	TMB	GEP*	Patient ID	Age	Sex	Tumor Type	TMB	GEP*
141	71	M	HNSCC	51	0.335	299	69	F	Melanoma	937	0.399
142	74	F	HNSCC	74	-0.319	300	57	M	Melanoma	61	-0.146
143	70	M	HNSCC	104	-0.103	301	73	F	Melanoma	198	0.205
144	51	M	HNSCC	122	-0.142	302	52	M	Melanoma	57	-0.453
145	63	F	HNSCC	342	0.142	303	43	M	Melanoma	740	0.235
146	63	M	HNSCC	77	-0.605	304	56	M	Melanoma	317	-0.046
147	62	M	HNSCC	31	-0.227	305	60	M	Melanoma	578	0.126
148	62	M	HNSCC	52	-0.227	306	56	M	Melanoma	421	0.308
149	50	M	HNSCC	590	-0.014	307	38	M	Melanoma	340	0.401
150	74	M	HNSCC	75	-0.372	308	55	M	Melanoma	1388	0.011
151	57	M	HNSCC	136	-0.053	309	47	F	Melanoma	59	0.201
152	69	M	HNSCC	350	-0.485	310	68	F	Melanoma	24	-0.157
153	66	M	HNSCC	46	0.094	311	42	F	Melanoma	33	-0.338
154	62	M	HNSCC Exp	48	0.053	312	60	M	Melanoma	233	-0.327
155	49	M	HNSCC Exp	129	0.090	313	51	M	Melanoma	557	-0.051
156	71	M	HNSCC Exp	93	0.093	314	45	F	Melanoma	37	-0.021
157	54	M	HNSCC Exp	72	-0.131	315	46	M	Melanoma	425	0.150
158	60	F	HNSCC Exp	267	0.135	-	-	-	-	-	-

Adeno=Adenocarcinoma; ER+HER- Breast= Estrogen Receptor Positive Human Epidermal Growth Factor Receptor-2 Negative Breast Cancer; Ext=extension study; PNET=pancreatic neuroendocrine tumors; SCC=squamous cell carcinoma; TNBC=triple-negative breast cancer. *GEP scores were calculated using gene data listed in Table S2B. †Papillary/Follicular; ‡ Gallbladder+Biliary Tree, excluding Ampulla of Vater; § Well/moderately differentiated PNET; ¶ Malignant Pleural; †† Including GE Junction

Patient ID	Housekeeping Genes										Predictor Genes																		
	STK11P	ZBTB34	TBC1D10B	OAZ1	POLR2A	G6PD	ABCF1	C14orf102	UBB	TBP	SDHA	CCL5	CD27	CD274	CD276	CD8A	CMKLR1	CXCL9	CXCR6	HLA.DQA1	HLA.DRB1	HLA.E	IDO1	LAG3	NGK7	PDCD1LG2	PSMB10	STAT1	TIGIT
305	83	110	113	3087	932	381	335	102	4675	128	1579	165	523	64	1124	144	178	451	29	2019	7301	5772	166	93	153	50	327	2718	285
306	151	491	213	5857	1404	489	561	102	9594	363	2259	1339	1476	116	493	485	381	2171	175	10249	19873	7168	659	270	1913	119	712	3734	685
307	63	121	107	2846	938	432	516	55	5907	131	1050	1224	416	53	1159	547	374	1274	203	2645	8048	5659	132	493	953	63	381	2976	223
308	78	171	76	2460	539	395	287	66	2212	157	808	289	135	54	751	128	351	939	36	13	992	3666	87	78	198	94	155	1479	63
309	53	26	10	127	201	68	52	25	171	33	351	56	196	23	42	87	52	35	7	852	1419	503	116	28	42	5	131	181	24
310	10	12	2	99	98	59	24	7	290	8	508	24	24	7	89	18	17	24	2	9	84	228	10	5	17	3	16	88	4
311	28	129	48	1117	368	126	294	27	4088	32	494	90	32	21	506	18	22	186	4	339	513	722	70	19	27	8	57	846	18
312	173	259	222	5547	995	961	802	154	7321	455	1682	276	69	68	3667	145	172	1241	41	1722	3091	5047	118	79	193	65	215	2569	73
313	174	192	168	6477	1382	414	582	129	8524	230	1827	519	99	117	1256	179	289	727	43	6313	7009	5413	209	97	299	56	336	4071	85
314	40	81	39	1521	307	143	135	41	1854	76	396	126	196	43	279	84	101	134	8	6	532	1729	139	43	75	33	123	569	59
315	66	144	86	2475	907	324	615	93	4741	119	1558	547	112	64	1040	319	221	3878	57	1085	5585	4268	458	106	322	57	180	1975	123

STK11P = Serine/threonine-protein kinase 11-interacting protein; ZBTB34 = Zinc finger and BTB domain-containing protein 34; TBC1D10B = TBC1 domain family member 10B; OAZ1 = Ornithine decarboxylase antizyme 1; POLR2A = DNA-directed RNA polymerase II subunit RPB1; G6PD = glucose-6-phosphate dehydrogenase; ABCF1 = ATP-binding cassette sub-family F member 1; C14orf102 = Chromosome 14 open reading frame 102-like protein; UBB = Ubiquitin; TBP = TATA-box binding protein; SDHA = succinate dehydrogenase complex flavoprotein subunit A; CCL5 = Chemokine (C-C motif) ligand 5; CD27 = CD27L receptor; PD-L1 (CD274) = programmed death ligand 1, CD274 molecule; CD276 (B7-H3) = CD276 antigen; CD8A = Cluster of differentiation 8a; CMKLR1 = Chemokine-like receptor 1; CXCL9 = Chemokine C-X-C motif ligand 9; CXCR6 = Chemokine C-X-C motif receptor 6; HLA.DQA1 = Major histocompatibility complex class II DQ alpha 1; HLA.DRB1 = Major histocompatibility complex class II DR beta 1; HLA.E = Major histocompatibility complex class I E;IDO1 = Indoleamine 2-3-dioxygenase 1; LAG3 = Lymphocyte-activation gene 3; NKG7 = Natural killer cell group 7 sequence; PDL2 (PDCD1LG2) = Programmed cell death 1 ligand 2; PSMB10 = Proteasome subunit beta type 10; STAT1 = Signal transducer and activator of transcription 1; TIGIT = T cell immunoreceptor with Ig and ITIM domains. GEP scores listed in Table S2A were computed by first normalizing the raw counts by subtracting the average of the log10 counts of the house-keeping genes from the log10 count of each of the predictor genes, and then a weighted sum of the normalized predictor gene values was calculated using the weights for each of the 18 genes (CCL5=0.008346; CD27=0.072293; CD274=0.042853; CD276=-0.0239; CD8A=0.031021; CMKLR1=0.151253; CXCL9=0.074135; CXCR6=0.004313; HLA.DQA1=0.020091; HLA.DRB1=0.058806; HLA.E=0.07175; IDO1=0.060679; LAG3=0.123895; NKG7=0.075524; PDCD1LG2=0.003734; PSMB10=0.032999; STAT1=0.250229; TIGIT=0.084767).

Table S3.

Tumor types and dominant mutational signatures in BOR Analysis

Study #	Cohort	Total (N)	Responders (n)	Dominant mutational signature (tumors with high TMB)	
KN028	Colon or rectal	5	0	Low TMB	
	Anal	8	2	APOBEC	
	Pancreas	2	0	Low TMB	
	Esophageal	3	1	Low TMB	
	Biliary	6	2	MMR	
	Carcinoid	6	0	Other	
	Neuroendocrine	1	0	Low TMB	
	ER ⁺ HER2 ⁻ Breast	2	0	HRD	
	Endometrial	4	1	POLE	
	Cervical	3	0	APOBEC	
	Vulvar	3	0	APOBEC	
	Small cell lung cancer	4	0	Smoking	
	Mesothelioma	9	1	Other	
	Thyroid	9	1	Other	
	Salivary gland	10	1	APOBEC	
	Leiomyosarcoma	2	0	Smoking	
	Prostate	3	1	MMR	
	KN012	Gastric	10	2	MMR
		TNBC	12	1	HRD
		Bladder	17	3	APOBEC
KN028/012	Combined	119	16	Heterogeneous	
KN012	HNSCC	107	21	APOBEC	
KN001, 006	Melanoma	89	38	UV exposure	
	All combined cohorts	315	75	Heterogeneous	
<p>The major mutational signatures displayed above as previously reported are the dominant signatures identified in the patient samples in this dataset (16). APOBEC=apolipoprotein B mRNA editing enzyme, catalytic polypeptide-like; ER=estrogen receptor; HER2=human epidermal growth factor 2; HNSCC=head and neck squamous cell carcinoma; HRD=homologous recombination deficiency; MMR=DNA mismatch repair; POLE=DNA polymerase epsilon catalytic subunit; TMB=tumor mutational burden; TNBC=triple negative breast cancer</p>					

Table S4.

Association of mutational signatures with BOR and PFS in pan-tumor cohort

Measure of Mutation	One-sided Nominal <i>P</i> -values	
	All subjects as treated	
	BOR N = 119	PFS N = 119
WES TMB (log scale)	0.001	0.017
DNA repair panel including HRD (any vs no mutation in panel)	0.037	0.155
Neoantigen signature (HLA-A,B binding <50nM, log-scale)	0.001	0.021
Smoking signature (log scale)	0.001	0.018
TP53 mutation	0.637	0.030
Fraction of APOBEC- driven mutations	0.226	0.319
Specific nucleotide change: sum C to A	0.144	0.119
Specific nucleotide change: sum C to G	0.102	0.116
Specific nucleotide change: sum C to T	0.004	0.020
Specific nucleotide change: sum T to A	0.008	0.041
Specific nucleotide change: sum T to C	0.029	0.056
Specific nucleotide change: sum T to G	0.015	0.052
<p>APOBEC=apolipoprotein B mRNA editing enzyme; HLA=human leukocyte antigen; HRD=Homologous recombination deficiency; TMB=tumor mutational burden; WES=whole exome sequencing. Logistic regression testing and Cox models were used for BOR and PFS, respectively. Models included terms for study (KN012/KN028) and baseline ECOG status (0 versus ≥ 1). APOBEC assessed only in Anal, Bladder, Breast and Cervical cancers. All mutational measures were tested for association with increased BOR and PFS, with the exception of TP53.</p>		

Table S5.

Gene enrichment in Sets 1 and 2

Genes with correlations >0.6

Keyword	Source	Pvalue	Evalue
Allograft Rejection Signaling (445lc)	IngenuityPathways	2.89E-42	5.25E-38
Immune response_Inhibitory PD-1 signaling in T cells	GeneGo	5.16E-41	9.38E-37
Immune response_Differentiation and clonal expansion of CD8+ T cells	GeneGo	2.94E-39	5.35E-35
NK cells in allergic contact dermatitis	GeneGo	4.49E-39	8.16E-35
Immune response_Immunological synapse formation	GeneGo	8.08E-38	1.47E-33
Immune response_Th1 and Th2 cell differentiation	GeneGo	2.16E-37	3.93E-33

Genes with correlations >0.15 and <0.6

Keyword	Source	Pvalue	Evalue
Role of Macrophages_ Fibroblasts and Endothelial Cells in Rheumatoid Arthritis (4ctnm)	IngenuityPathways	1.04E-27	1.89E-23
TREM1 Signaling (3j6wq)	IngenuityPathways	3.36E-26	6.10E-22
Cell adhesion_Chemokines and adhesion	GeneGo	6.94E-25	1.26E-20
Granulocyte Adhesion and Diapedesis (8tsni)	IngenuityPathways	1.03E-24	1.87E-20
Agranulocyte Adhesion and Diapedesis (8tsnh)	IngenuityPathways	1.80E-23	3.28E-19
Cytokine-cytokine receptor interaction	kegg	9.87E-23	1.79E-18
B Cell Receptor Signaling (cil)	IngenuityPathways	1.96E-19	3.57E-15
Immune response_Inflammasome in inflammatory response	GeneGo	2.13E-19	3.87E-15
Atherosclerosis Signaling (4ctne)	IngenuityPathways	2.82E-19	5.13E-15
Release of pro-inflammatory factors and proteases by alveolar macrophages in asthma	GeneGo	2.93E-19	5.32E-15
Hepatic Fibrosis _ Hepatic Stellate Cell Activation (1nilk)	IngenuityPathways	7.50E-19	1.36E-14
Cell adhesion_ECM remodeling	GeneGo	1.57E-18	2.85E-14
Role of Pattern Recognition Receptors in Recognition of Bacteria and Viruses (3j6wo)	IngenuityPathways	1.58E-18	2.88E-14

Table S6.
General group annotation of genes in modules

General annotation	
1	Anti-bacterial defense
2	ECM remodeling
3	Keratins and MMPs
4	Proliferation
5	Vasculature
6	Wound healing
7	PMNs
8	B-cell receptor (I)
9	B-cell receptor (II)
10	Cytoskeleton remodeling

Table S7.

Gene annotation (TCGA database)

Annotation of genes with average correlation with TMB in GEP+ <-0.21425 genes: Key annotation (cell cyc, kegg, Ingenuity, genego): **Vasculature**

Name	Source	EValue	PValue
Vascular smooth muscle contraction	kegg	1.50E-05	8.08E-09
GABA Receptor Signaling (cih)	Ingenuity	6.70E-05	3.66E-08
Development_Alpha-1 adrenergic receptors signaling via cAMP	GeneGo	0.00011	5.84E-08
Cellular Effects of Sildenafil Viagra (3v731)	Ingenuity	0.00014	7.86E-08
Role of NFAT in Cardiac Hypertrophy (4uiun)	Ingenuity	0.00018	9.92E-08
Muscle contraction_GPCRs in the regulation of smooth muscle tone	GeneGo	0.00019	1.06E-07
G-Protein Coupled Receptor Signaling (cj8)	Ingenuity	0.00052	2.84E-07
Relaxin Signaling (3v73l)	Ingenuity	0.00068	3.73E-07
Regulation of intrinsic membrane properties and excitability of cortical pyramidal neurons	GeneGo	0.00083	4.57E-07

Annotation of genes with average correlation with TMB in GEP+ >0.21921 genes: Key annotation (cell cyc, kegg, Ingenuity, genego): **Cell cycle (proliferation)**

Name	Source	EValue	PValue
G2	cellcyc	7.00E-22	3.83E-25
G2/M	cellcyc	3.30E-21	1.81E-24
Cell cycle_The metaphase checkpoint	GeneGo	6.50E-20	3.58E-23
Cell cycle_Role of APC in cell cycle regulation	GeneGo	1.30E-17	7.37E-21
Cell cycle_Transition and termination of DNA replication	GeneGo	6.00E-17	3.28E-20
HSP70 and HSP40-dependent folding in Huntington's disease	GeneGo	6.80E-15	3.73E-18
Putative pathways of MHC class I-dependent postsynaptic long-term depression in major depressive disorder	GeneGo	1.20E-14	6.30E-18
DNA replication	kegg	3.60E-14	1.99E-17
Immune response_Antigen presentation by MHC class I	GeneGo	1.20E-13	6.41E-17
Ubiquitin-proteasome system in Huntington's disease	GeneGo	2.70E-13	1.46E-16
Cell cycle	kegg	9.30E-13	5.08E-16

References and Notes

1. S. J. Lee, B.-C. Jang, S.-W. Lee, Y.-I. Yang, S.-I. Suh, Y.-M. Park, S. Oh, J.-G. Shin, S. Yao, L. Chen, I.-H. Choi, Interferon regulatory factor-1 is prerequisite to the constitutive expression and IFN-gamma-induced upregulation of B7-H1 (CD274). *FEBS Lett.* **580**, 755–762 (2006). [doi:10.1016/j.febslet.2005.12.093](https://doi.org/10.1016/j.febslet.2005.12.093) [Medline](#)
2. C. Lu, P. S. Redd, J. R. Lee, N. Savage, K. Liu, The expression profiles and regulation of PD-L1 in tumor-induced myeloid-derived suppressor cells. *Oncoimmunology* **5**, e1247135 (2016). [doi:10.1080/2162402X.2016.1247135](https://doi.org/10.1080/2162402X.2016.1247135) [Medline](#)
3. J. M. Taube, A. Klein, J. R. Brahmer, H. Xu, X. Pan, J. H. Kim, L. Chen, D. M. Pardoll, S. L. Topalian, R. A. Anders, Association of PD-1, PD-1 ligands, and other features of the tumor immune microenvironment with response to anti-PD-1 therapy. *Clin. Cancer Res.* **20**, 5064–5074 (2014). [doi:10.1158/1078-0432.CCR-13-3271](https://doi.org/10.1158/1078-0432.CCR-13-3271) [Medline](#)
4. A. Snyder, V. Makarov, T. Merghoub, J. Yuan, J. M. Zaretsky, A. Desrichard, L. A. Walsh, M. A. Postow, P. Wong, T. S. Ho, T. J. Hollmann, C. Bruggeman, K. Kannan, Y. Li, C. Elipenahli, C. Liu, C. T. Harbison, L. Wang, A. Ribas, J. D. Wolchok, T. A. Chan, Genetic basis for clinical response to CTLA-4 blockade in melanoma. *N. Engl. J. Med.* **371**, 2189–2199 (2014). [doi:10.1056/NEJMoa1406498](https://doi.org/10.1056/NEJMoa1406498) [Medline](#)
5. E. M. Van Allen, D. Miao, B. Schilling, S. A. Shukla, C. Blank, L. Zimmer, A. Sucker, U. Hillen, M. H. G. Foppen, S. M. Goldinger, J. Utikal, J. C. Hassel, B. Weide, K. C. Kaehler, C. Loquai, P. Mohr, R. Gutzmer, R. Dummer, S. Gabriel, C. J. Wu, D. Schadendorf, L. A. Garraway, Genomic correlates of response to CTLA-4 blockade in metastatic melanoma. *Science* **350**, 207–211 (2015). [doi:10.1126/science.aad0095](https://doi.org/10.1126/science.aad0095) [Medline](#)
6. W. Hugo, J. M. Zaretsky, L. Sun, C. Song, B. H. Moreno, S. Hu-Lieskovan, B. Berent-Maoz, J. Pang, B. Chmielowski, G. Cherry, E. Seja, S. Lomeli, X. Kong, M. C. Kelley, J. A. Sosman, D. B. Johnson, A. Ribas, R. S. Lo, Genomic and transcriptomic features of response to anti-PD-1 therapy in metastatic melanoma. *Cell* **165**, 35–44 (2016). [doi:10.1016/j.cell.2016.02.065](https://doi.org/10.1016/j.cell.2016.02.065) [Medline](#)
7. D. B. Johnson, M. H. Pollack, J. A. Sosman, Emerging targeted therapies for melanoma. *Expert Opin. Emerg. Drugs* **21**, 195–207 (2016). [doi:10.1080/14728214.2016.1184644](https://doi.org/10.1080/14728214.2016.1184644) [Medline](#)
8. N. A. Rizvi, M. D. Hellmann, A. Snyder, P. Kvistborg, V. Makarov, J. J. Havel, W. Lee, J. Yuan, P. Wong, T. S. Ho, M. L. Miller, N. Rekhtman, A. L. Moreira, F. Ibrahim, C. Bruggeman, B. Gasmi, R. Zappasodi, Y. Maeda, C. Sander, E. B. Garon, T. Merghoub, J. D. Wolchok, T. N. Schumacher, T. A. Chan, Mutational landscape determines sensitivity to PD-1 blockade in non-small cell lung cancer. *Science* **348**, 124–128 (2015). [doi:10.1126/science.aaa1348](https://doi.org/10.1126/science.aaa1348) [Medline](#)
9. M. Kowanetz, W. Zou, D. S. Shames, C. Cummings, N. Rizvi, A. I. Spira, G. M. Frampton, V. Leveque, S. Flynn, S. Mocci, G. Shankar, R. Funke, M. Ballinger, D. Waterkamp, A. Sandler, G. Hampton, L. Amler, P. S. Hegde, M. Hellmann, Tumor mutation load assessed by FoundationOne (FM1) is associated with improved efficacy of atezolizumab

- (atezo) in patients with advanced NSCLC. *Ann. Oncol.* **27**, 77P (2016).
[doi:10.1093/annonc/mdw363.25](https://doi.org/10.1093/annonc/mdw363.25)
10. D. T. Le, J. N. Durham, K. N. Smith, H. Wang, B. R. Bartlett, L. K. Aulakh, S. Lu, H. Kemberling, C. Wilt, B. S. Lubner, F. Wong, N. S. Azad, A. A. Rucki, D. Laheru, R. Donehower, A. Zaheer, G. A. Fisher, T. S. Crocenzi, J. J. Lee, T. F. Greten, A. G. Duffy, K. K. Ciombor, A. D. Eyring, B. H. Lam, A. Joe, S. P. Kang, M. Holdhoff, L. Danilova, L. Cope, C. Meyer, S. Zhou, R. M. Goldberg, D. K. Armstrong, K. M. Bever, A. N. Fader, J. Taube, F. Housseau, D. Spetzler, N. Xiao, D. M. Pardoll, N. Papadopoulos, K. W. Kinzler, J. R. Eshleman, B. Vogelstein, R. A. Anders, L. A. Diaz Jr., Mismatch repair deficiency predicts response of solid tumors to PD-1 blockade. *Science* **357**, 409–413 (2017). [doi:10.1126/science.aan6733](https://doi.org/10.1126/science.aan6733) [Medline](#)
 11. D. T. Le, J. N. Uram, H. Wang, B. R. Bartlett, H. Kemberling, A. D. Eyring, A. D. Skora, B. S. Lubner, N. S. Azad, D. Laheru, B. Biedrzycki, R. C. Donehower, A. Zaheer, G. A. Fisher, T. S. Crocenzi, J. J. Lee, S. M. Duffy, R. M. Goldberg, A. de la Chapelle, M. Koshiji, F. Bhajee, T. Huebner, R. H. Hruban, L. D. Wood, N. Cuka, D. M. Pardoll, N. Papadopoulos, K. W. Kinzler, S. Zhou, T. C. Cornish, J. M. Taube, R. A. Anders, J. R. Eshleman, B. Vogelstein, L. A. Diaz Jr., PD-1 blockade in tumors with mismatch-repair deficiency. *N. Engl. J. Med.* **372**, 2509–2520 (2015). [doi:10.1056/NEJMoa1500596](https://doi.org/10.1056/NEJMoa1500596) [Medline](#)
 12. J. E. Rosenberg, J. Hoffman-Censits, T. Powles, M. S. van der Heijden, A. V. Balar, A. Necchi, N. Dawson, P. H. O'Donnell, A. Balmanoukian, Y. Loriot, S. Srinivas, M. M. Retz, P. Grivas, R. W. Joseph, M. D. Galsky, M. T. Fleming, D. P. Petrylak, J. L. Perez-Gracia, H. A. Burris, D. Castellano, C. Canil, J. Bellmunt, D. Bajorin, D. Nickles, R. Bourgon, G. M. Frampton, N. Cui, S. Mariathasan, O. Abidoye, G. D. Fine, R. Dreicer, Atezolizumab in patients with locally advanced and metastatic urothelial carcinoma who have progressed following treatment with platinum-based chemotherapy: A single-arm, multicentre, phase 2 trial. *Lancet* **387**, 1909–1920 (2016). [doi:10.1016/S0140-6736\(16\)00561-4](https://doi.org/10.1016/S0140-6736(16)00561-4) [Medline](#)
 13. M. S. Rooney, S. A. Shukla, C. J. Wu, G. Getz, N. Hacohen, Molecular and genetic properties of tumors associated with local immune cytolytic activity. *Cell* **160**, 48–61 (2015). [doi:10.1016/j.cell.2014.12.033](https://doi.org/10.1016/j.cell.2014.12.033) [Medline](#)
 14. P. C. Tumeh, C. L. Harview, J. H. Yearley, I. P. Shintaku, E. J. M. Taylor, L. Robert, B. Chmielowski, M. Spasic, G. Henry, V. Ciobanu, A. N. West, M. Carmona, C. Kivork, E. Seja, G. Cherry, A. J. Gutierrez, T. R. Grogan, C. Mateus, G. Tomasic, J. A. Glaspy, R. O. Emerson, H. Robins, R. H. Pierce, D. A. Elashoff, C. Robert, A. Ribas, PD-1 blockade induces responses by inhibiting adaptive immune resistance. *Nature* **515**, 568–571 (2014). [doi:10.1038/nature13954](https://doi.org/10.1038/nature13954) [Medline](#)
 15. M. Ayers, J. Lunceford, M. Nebozhyn, E. Murphy, A. Loboda, D. R. Kaufman, A. Albright, J. D. Cheng, S. P. Kang, V. Shankaran, S. A. Piha-Paul, J. Yearley, T. Y. Seiwert, A. Ribas, T. K. McClanahan, IFN- γ -related mRNA profile predicts clinical response to PD-1 blockade. *J. Clin. Invest.* **127**, 2930–2940 (2017). [doi:10.1172/JCI91190](https://doi.org/10.1172/JCI91190) [Medline](#)
 16. The Cancer Genome Atlas, TCGA Data Portal; <https://tcga-data.nci.nih.gov/docs/publications/tcga/>.

17. L. B. Alexandrov, M. R. Stratton, Mutational signatures: The patterns of somatic mutations hidden in cancer genomes. *Curr. Opin. Genet. Dev.* **24**, 52–60 (2014).
[doi:10.1016/j.gde.2013.11.014](https://doi.org/10.1016/j.gde.2013.11.014) [Medline](#)
18. R. Haddad, T. Y. Seiwert, L. Q. M. Chow, S. Gupta, J. Weiss, I. Gluck, J. P. Eder, B. Burtneess, M. Tahara, B. Keam, H. Kang, K. Muro, A. Albright, L. Huang, M. Ayers, R. Mogg, R. Cristescu, J. D. Cheng, R. Mehra, Genomic determinants of response to pembrolizumab in head and neck squamous cell carcinoma. *J. Clin. Oncol.* **35** (Suppl.), 6009 (2017). [doi:10.1200/JCO.2017.35.15_suppl.6009](https://doi.org/10.1200/JCO.2017.35.15_suppl.6009)
19. D. B. Johnson, G. M. Frampton, M. J. Rioth, E. Yusko, Y. Xu, X. Guo, R. C. Ennis, D. Fabrizio, Z. R. Chalmers, J. Greenbowe, S. M. Ali, S. Balasubramanian, J. X. Sun, Y. He, D. T. Frederick, I. Puzanov, J. M. Balko, J. M. Cates, J. S. Ross, C. Sanders, H. Robins, Y. Shyr, V. A. Miller, P. J. Stephens, R. J. Sullivan, J. A. Sosman, C. M. Lovly, Targeted next generation sequencing identifies markers of response to PD-1 blockade. *Cancer Immunol. Res.* **4**, 959–967 (2016). [doi:10.1158/2326-6066.CIR-16-0143](https://doi.org/10.1158/2326-6066.CIR-16-0143) [Medline](#)
20. A. Panda, A. Betigeri, K. Subramanian, J. S. Ross, D. C. Pavlick, S. Ali, P. Markowski, A. Silk, H. L. Kaufman, E. Lattime, J. M. Mehnert, R. Sullivan, C. M. Lovly, J. Sosman, D. B. Johnson, G. Bhanot, S. Ganesan, Identifying a clinically applicable mutational burden threshold as a potential biomarker of response to immune checkpoint therapy in solid tumors. *JCO Precis. Oncol.* **2017**, 10.1200/PO.17.00146 (2017). [Medline](#)
21. T. Y. Seiwert, R. Haddad, J. Bauml, J. Weiss, D. G. Pfister, S. Gupta, R. Mehra, I. Gluck, H. Kang, F. Worden, J. P. Eder, M. Tahara, B. Burtneess, S. V. Liu, A. Webber, L. Huang, R. Mogg, R. Cristescu, J. Cheng, L. Q. Chow, “Biomarkers predictive of response to pembrolizumab in head and neck cancer (HNSCC),” in *Proceedings of the American Association for Cancer Research Annual Meeting 2018*, Chicago, IL, 14 to 18 April 2018 (American Association for Cancer Research, 2018), abstract no. LB-339.
22. S. J. Salipante, S. M. Scroggins, H. L. Hampel, E. H. Turner, C. C. Pritchard, Microsatellite instability detection by next generation sequencing. *Clin. Chem.* **60**, 1192–1199 (2014).
[doi:10.1373/clinchem.2014.223677](https://doi.org/10.1373/clinchem.2014.223677) [Medline](#)
23. W. Roh, P.-L. Chen, A. Reuben, C. N. Spencer, P. A. Prieto, J. P. Miller, V. Gopalakrishnan, F. Wang, Z. A. Cooper, S. M. Reddy, C. Gumbs, L. Little, Q. Chang, W.-S. Chen, K. Wani, M. P. De Macedo, E. Chen, J. L. Austin-Breneman, H. Jiang, J. Roszik, M. T. Tetzlaff, M. A. Davies, J. E. Gershenwald, H. Tawbi, A. J. Lazar, P. Hwu, W.-J. Hwu, A. Diab, I. C. Glitza, S. P. Patel, S. E. Woodman, R. N. Amaria, V. G. Prieto, J. Hu, P. Sharma, J. P. Allison, L. Chin, J. Zhang, J. A. Wargo, P. A. Futreal, Integrated molecular analysis of tumor biopsies on sequential CTLA-4 and PD-1 blockade reveals markers of response and resistance. *Sci. Transl. Med.* **9**, eaah3560 (2017).
[doi:10.1126/scitranslmed.aah3560](https://doi.org/10.1126/scitranslmed.aah3560) [Medline](#)
24. N. McGranahan, A. J. S. Furness, R. Rosenthal, S. Ramskov, R. Lyngaa, S. K. Saini, M. Jamal-Hanjani, G. A. Wilson, N. J. Birkbak, C. T. Hiley, T. B. K. Watkins, S. Shafi, N. Murugaesu, R. Mitter, A. U. Akarca, J. Linares, T. Marafioti, J. Y. Henry, E. M. Van Allen, D. Miao, B. Schilling, D. Schadendorf, L. A. Garraway, V. Makarov, N. A. Rizvi, A. Snyder, M. D. Hellmann, T. Merghoub, J. D. Wolchok, S. A. Shukla, C. J. Wu, K. S. Peggs, T. A. Chan, S. R. Hadrup, S. A. Quezada, C. Swanton, Clonal neoantigens elicit T

- cell immunoreactivity and sensitivity to immune checkpoint blockade. *Science* **351**, 1463–1469 (2016). [doi:10.1126/science.aaf1490](https://doi.org/10.1126/science.aaf1490) [Medline](#)
25. E. B. Garon, N. A. Rizvi, R. Hui, N. Leighl, A. S. Balmanoukian, J. P. Eder, A. Patnaik, C. Aggarwal, M. Gubens, L. Horn, E. Carcereny, M.-J. Ahn, E. Felip, J.-S. Lee, M. D. Hellmann, O. Hamid, J. W. Goldman, J.-C. Soria, M. Dolled-Filhart, R. Z. Rutledge, J. Zhang, J. K. Luceford, R. Rangwala, G. M. Lubiniecki, C. Roach, K. Emancipator, L. Gandhi, KEYNOTE-001 Investigators, Pembrolizumab for the treatment of non-small-cell lung cancer. *N. Engl. J. Med.* **372**, 2018–2028 (2015). [doi:10.1056/NEJMoa1501824](https://doi.org/10.1056/NEJMoa1501824) [Medline](#)
 26. C. Robert, J. Schachter, G. V. Long, A. Arance, J. J. Grob, L. Mortier, A. Daud, M. S. Carlino, C. McNeil, M. Lotem, J. Larkin, P. Lorigan, B. Neyns, C. U. Blank, O. Hamid, C. Mateus, R. Shapira-Frommer, M. Kosh, H. Zhou, N. Ibrahim, S. Ebbinghaus, A. Ribas, KEYNOTE-006 Investigators, Pembrolizumab versus ipilimumab in advanced melanoma. *N. Engl. J. Med.* **372**, 2521–2532 (2015). [doi:10.1056/NEJMoa1503093](https://doi.org/10.1056/NEJMoa1503093) [Medline](#)
 27. M. R. Neagu, D. A. Reardon, An update on the role of immunotherapy and vaccine strategies for primary brain tumors. *Curr. Treat. Options Oncol.* **16**, 54 (2015). [doi:10.1007/s11864-015-0371-3](https://doi.org/10.1007/s11864-015-0371-3) [Medline](#)
 28. U. Vaishampayan, Therapeutic options and multifaceted treatment paradigms in metastatic castrate-resistant prostate cancer. *Curr. Opin. Oncol.* **26**, 265–273 (2014). [doi:10.1097/CCO.0000000000000066](https://doi.org/10.1097/CCO.0000000000000066) [Medline](#)
 29. D. Coppola, M. Nebozhyn, F. Khalil, H. Dai, T. Yeatman, A. Loboda, J. J. Mulé, Unique ectopic lymph node-like structures present in human primary colorectal carcinoma are identified by immune gene array profiling. *Am. J. Pathol.* **179**, 37–45 (2011). [doi:10.1016/j.ajpath.2011.03.007](https://doi.org/10.1016/j.ajpath.2011.03.007) [Medline](#)
 30. J. Galon, H. K. Angell, D. Bedognetti, F. M. Marincola, The continuum of cancer immunosurveillance: Prognostic, predictive, and mechanistic signatures. *Immunity* **39**, 11–26 (2013). [doi:10.1016/j.immuni.2013.07.008](https://doi.org/10.1016/j.immuni.2013.07.008) [Medline](#)
 31. M. Łuksza, N. Riaz, V. Makarov, V. P. Balachandran, M. D. Hellmann, A. Solovyov, N. A. Rizvi, T. Merghoub, A. J. Levine, T. A. Chan, J. D. Wolchok, B. D. Greenbaum, A neoantigen fitness model predicts tumour response to checkpoint blockade immunotherapy. *Nature* **551**, 517–520 (2017). [Medline](#)
 32. H. Dai, L. van't Veer, J. Lamb, Y. D. He, M. Mao, B. M. Fine, R. Bernards, M. van de Vijver, P. Deutsch, A. Sachs, R. Stoughton, S. Friend, A cell proliferation signature is a marker of extremely poor outcome in a subpopulation of breast cancer patients. *Cancer Res.* **65**, 4059–4066 (2005). [doi:10.1158/0008-5472.CAN-04-3953](https://doi.org/10.1158/0008-5472.CAN-04-3953) [Medline](#)
 33. S. Spranger, R. Bao, T. F. Gajewski, Melanoma-intrinsic β -catenin signalling prevents anti-tumour immunity. *Nature* **523**, 231–235 (2015). [doi:10.1038/nature14404](https://doi.org/10.1038/nature14404) [Medline](#)
 34. K. Yoshihara, M. Shahmoradgoli, E. Martínez, R. Vegesna, H. Kim, W. Torres-Garcia, V. Treviño, H. Shen, P. W. Laird, D. A. Levine, S. L. Carter, G. Getz, K. Stemke-Hale, G. B. Mills, R. G. W. Verhaak, Inferring tumour purity and stromal and immune cell

- admixture from expression data. *Nat. Commun.* **4**, 2612 (2013). [doi:10.1038/ncomms3612](https://doi.org/10.1038/ncomms3612) [Medline](#)
35. A. C. Huang, M. A. Postow, R. J. Orlowski, R. Mick, B. Bengsch, S. Manne, W. Xu, S. Harmon, J. R. Giles, B. Wenz, M. Adamow, D. Kuk, K. S. Panageas, C. Carrera, P. Wong, F. Quagliarello, B. Wubbenhorst, K. D'Andrea, K. E. Pauken, R. S. Herati, R. P. Staupé, J. M. Schenkel, S. McGettigan, S. Kothari, S. M. George, R. H. Vonderheide, R. K. Amaravadi, G. C. Karakousis, L. M. Schuchter, X. Xu, K. L. Nathanson, J. D. Wolchok, T. C. Gangadhar, E. J. Wherry, T-cell invigoration to tumour burden ratio associated with anti-PD-1 response. *Nature* **545**, 60–65 (2017). [doi:10.1038/nature22079](https://doi.org/10.1038/nature22079) [Medline](#)
 36. P. F. Robbins, Y.-C. Lu, M. El-Gamil, Y. F. Li, C. Gross, J. Gartner, J. C. Lin, J. K. Teer, P. Cliften, E. Tycksen, Y. Samuels, S. A. Rosenberg, Mining exomic sequencing data to identify mutated antigens recognized by adoptively transferred tumor-reactive T cells. *Nat. Med.* **19**, 747–752 (2013). [doi:10.1038/nm.3161](https://doi.org/10.1038/nm.3161) [Medline](#)
 37. N. H. Segal, D. W. Parsons, K. S. Peggs, V. Velculescu, K. W. Kinzler, B. Vogelstein, J. P. Allison, Epitope landscape in breast and colorectal cancer. *Cancer Res.* **68**, 889–892 (2008). [doi:10.1158/0008-5472.CAN-07-3095](https://doi.org/10.1158/0008-5472.CAN-07-3095) [Medline](#)
 38. H. Matsushita, M. D. Vesely, D. C. Koboldt, C. G. Rickert, R. Uppaluri, V. J. Magrini, C. D. Arthur, J. M. White, Y.-S. Chen, L. K. Shea, J. Hundal, M. C. Wendl, R. Demeter, T. Wylie, J. P. Allison, M. J. Smyth, L. J. Old, E. R. Mardis, R. D. Schreiber, Cancer exome analysis reveals a T-cell-dependent mechanism of cancer immunoediting. *Nature* **482**, 400–404 (2012). [doi:10.1038/nature10755](https://doi.org/10.1038/nature10755) [Medline](#)
 39. M. Dolled-Filhart, C. Roach, G. Toland, D. Stanforth, M. Jansson, G. M. Lubiniecki, G. Ponto, K. Emancipator, Development of a companion diagnostic for pembrolizumab in non-small cell lung cancer using immunohistochemistry for programmed death ligand-1. *Arch. Pathol. Lab. Med.* **140**, 1243–1249 (2016). [doi:10.5858/arpa.2015-0542-OA](https://doi.org/10.5858/arpa.2015-0542-OA) [Medline](#)
 40. L. Q. Chow, B. Burtneß, J. Weiss, R. Berger, J. P. Eder, E. J. Gonzalez, J. Pulini, J. Johnson, M. Dolled-Filhart, K. Emancipator, J. K. Luceford, K. Pathiraja, C. Gause, J. D. Cheng, T. Seiwert, A phase Ib study of pembrolizumab (pembro; MK-3475) in patients (pts) with human papillomavirus virus (HPV)-positive and negative head and neck cancer (HNC). *Ann. Oncol.* **25** (Suppl. 4), 14 (2014). [doi:10.1093/annonc/mdu438.32](https://doi.org/10.1093/annonc/mdu438.32)
 41. T. Y. Seiwert, B. Burtneß, R. Mehra, J. Weiss, R. Berger, J. P. Eder, K. Heath, T. McClanahan, J. Luceford, C. Gause, J. D. Cheng, L. Q. Chow, Safety and clinical activity of pembrolizumab for treatment of recurrent or metastatic squamous cell carcinoma of the head and neck (KEYNOTE-012): An open-label, multicentre, phase 1b trial. *Lancet Oncol.* **17**, 956–965 (2016). [doi:10.1016/S1470-2045\(16\)30066-3](https://doi.org/10.1016/S1470-2045(16)30066-3) [Medline](#)
 42. O. Hamid, C. Robert, A. Daud, F. S. Hodi, W.-J. Hwu, R. Kefford, J. D. Wolchok, P. Hersey, R. W. Joseph, J. S. Weber, R. Dronca, T. C. Gangadhar, A. Patnaik, H. Zarour, A. M. Joshua, K. Gergich, J. Ellassaïss-Schaap, A. Algazi, C. Mateus, P. Boasberg, P. C. Tumeh, B. Chmielowski, S. W. Ebbinghaus, X. N. Li, S. P. Kang, A. Ribas, Safety and tumor responses with lambrolizumab (anti-PD-1) in melanoma. *N. Engl. J. Med.* **369**, 134–144 (2013). [doi:10.1056/NEJMoa1305133](https://doi.org/10.1056/NEJMoa1305133) [Medline](#)

43. H. Li, R. Durbin, Fast and accurate short read alignment with Burrows-Wheeler transform. *Bioinformatics* **25**, 1754–1760 (2009). [doi:10.1093/bioinformatics/btp324](https://doi.org/10.1093/bioinformatics/btp324) [Medline](#)
44. A. McKenna, M. Hanna, E. Banks, A. Sivachenko, K. Cibulskis, A. Kernytsky, K. Garimella, D. Altshuler, S. Gabriel, M. Daly, M. A. DePristo, The Genome Analysis Toolkit: A MapReduce framework for analyzing next-generation DNA sequencing data. *Genome Res.* **20**, 1297–1303 (2010). [doi:10.1101/gr.107524.110](https://doi.org/10.1101/gr.107524.110) [Medline](#)
45. K. Cibulskis, M. S. Lawrence, S. L. Carter, A. Sivachenko, D. Jaffe, C. Sougnez, S. Gabriel, M. Meyerson, E. S. Lander, G. Getz, Sensitive detection of somatic point mutations in impure and heterogeneous cancer samples. *Nat. Biotechnol.* **31**, 213–219 (2013). [doi:10.1038/nbt.2514](https://doi.org/10.1038/nbt.2514) [Medline](#)
46. S. T. Sherry, M. Ward, K. Sirotkin, dbSNP-database for single nucleotide polymorphisms and other classes of minor genetic variation. *Genome Res.* **9**, 677–679 (1999). [Medline](#)
47. S. A. Forbes, G. Tang, N. Bindal, S. Bamford, E. Dawson, C. Cole, C. Y. Kok, M. Jia, R. Ewing, A. Menzies, J. W. Teague, M. R. Stratton, P. A. Futreal, COSMIC (the Catalogue of Somatic Mutations in Cancer): A resource to investigate acquired mutations in human cancer. *Nucleic Acids Res.* **38**, D652–D657 (2010). [doi:10.1093/nar/gkp995](https://doi.org/10.1093/nar/gkp995) [Medline](#)
48. A. Szolek, B. Schubert, C. Mohr, M. Sturm, M. Feldhahn, O. Kohlbacher, OptiType: Precision HLA typing from next-generation sequencing data. *Bioinformatics* **30**, 3310–3316 (2014). [doi:10.1093/bioinformatics/btu548](https://doi.org/10.1093/bioinformatics/btu548) [Medline](#)
49. M. Nielsen, C. Lundegaard, P. Worning, S. L. Lauemøller, K. Lamberth, S. Buus, S. Brunak, O. Lund, Reliable prediction of T-cell epitopes using neural networks with novel sequence representations. *Protein Sci.* **12**, 1007–1017 (2003). [doi:10.1110/ps.0239403](https://doi.org/10.1110/ps.0239403) [Medline](#)
50. O. Lund, M. Nielsen, C. Kesmir, A. G. Petersen, C. Lundegaard, P. Worning, C. Sylvester-Hvid, K. Lamberth, G. Røder, S. Justesen, S. Buus, S. Brunak, Definition of supertypes for HLA molecules using clustering of specificity matrices. *Immunogenetics* **55**, 797–810 (2004). [doi:10.1007/s00251-004-0647-4](https://doi.org/10.1007/s00251-004-0647-4) [Medline](#)
51. J. Sidney, B. Peters, N. Frahm, C. Brander, A. Sette, HLA class I supertypes: A revised and updated classification. *BMC Immunol.* **9**, 1 (2008). [doi:10.1186/1471-2172-9-1](https://doi.org/10.1186/1471-2172-9-1) [Medline](#)
52. W. McLaren, L. Gil, S. E. Hunt, H. S. Riat, G. R. S. Ritchie, A. Thormann, P. Flicek, F. Cunningham, The Ensembl Variant Effect Predictor. *Genome Biol.* **17**, 122 (2016). [doi:10.1186/s13059-016-0974-4](https://doi.org/10.1186/s13059-016-0974-4) [Medline](#)
53. R. Rosenthal, N. McGranahan, J. Herrero, B. S. Taylor, C. Swanton, DeconstructSigs: Delineating mutational processes in single tumors distinguishes DNA repair deficiencies and patterns of carcinoma evolution. *Genome Biol.* **17**, 31 (2016). [doi:10.1186/s13059-016-0893-4](https://doi.org/10.1186/s13059-016-0893-4) [Medline](#)
54. L. B. Alexandrov, S. Nik-Zainal, D. C. Wedge, S. A. J. R. Aparicio, S. Behjati, A. V. Biankin, G. R. Bignell, N. Bolli, A. Borg, A.-L. Børresen-Dale, S. Boyault, B. Burkhardt, A. P. Butler, C. Caldas, H. R. Davies, C. Desmedt, R. Eils, J. E. Eyfjörd, J. A. Foekens, M. Greaves, F. Hosoda, B. Hutter, T. Ilcic, S. Imbeaud, M. Imielinski, N. Jäger, D. T. W. Jones, D. Jones, S. Knappskog, M. Kool, S. R. Lakhani, C. López-Otín, S. Martin, N. C. Munshi, H. Nakamura, P. A. Northcott, M. Pajic, E. Papaemmanuil, A. Paradiso, J. V.

- Pearson, X. S. Puente, K. Raine, M. Ramakrishna, A. L. Richardson, J. Richter, P. Rosenstiel, M. Schlesner, T. N. Schumacher, P. N. Span, J. W. Teague, Y. Totoki, A. N. J. Tutt, R. Valdés-Mas, M. M. van Buuren, L. van 't Veer, A. Vincent-Salomon, N. Waddell, L. R. Yates, J. Zucman-Rossi, P. A. Futreal, U. McDermott, P. Lichter, M. Meyerson, S. M. Grimmond, R. Siebert, E. Campo, T. Shibata, S. M. Pfister, P. J. Campbell, M. R. Stratton, Australian Pancreatic Cancer Genome Initiative, ICGC Breast Cancer Consortium, ICGC MMML-Seq Consortium, ICGC PedBrain, Signatures of mutational processes in human cancer. *Nature* **500**, 415–421 (2013). [doi:10.1038/nature12477](https://doi.org/10.1038/nature12477) [Medline](#)
55. D. C. Koboldt, Q. Zhang, D. E. Larson, D. Shen, M. D. McLellan, L. Lin, C. A. Miller, E. R. Mardis, L. Ding, R. K. Wilson, VarScan 2: Somatic mutation and copy number alteration discovery in cancer by exome sequencing. *Genome Res.* **22**, 568–576 (2012). [doi:10.1101/gr.129684.111](https://doi.org/10.1101/gr.129684.111) [Medline](#)
56. F. Favero, T. Joshi, A. M. Marquard, N. J. Birkbak, M. Krzystanek, Q. Li, Z. Szallasi, A. C. Eklund, Sequenza: Allele-specific copy number and mutation profiles from tumor sequencing data. *Ann. Oncol.* **26**, 64–70 (2015). [doi:10.1093/annonc/mdu479](https://doi.org/10.1093/annonc/mdu479) [Medline](#)
57. A. Roth, J. Khattra, D. Yap, A. Wan, E. Laks, J. Biele, G. Ha, S. Aparicio, A. Bouchard-Côté, S. P. Shah, PyClone: Statistical inference of clonal population structure in cancer. *Nat. Methods* **11**, 396–398 (2014). [doi:10.1038/nmeth.2883](https://doi.org/10.1038/nmeth.2883) [Medline](#)
58. M. Dolled-Filhart, D. Locke, T. Murphy, F. Lynch, J. H. Yearley, D. Frisman, R. Pierce, R. Weiner, D. Wu, K. Emancipator, Development of a prototype immunohistochemistry assay to measure programmed death ligand-1 expression in tumor tissue. *Arch. Pathol. Lab. Med.* **140**, 1259–1266 (2016). [doi:10.5858/arpa.2015-0544-OA](https://doi.org/10.5858/arpa.2015-0544-OA) [Medline](#)
59. A. I. Daud, J. D. Wolchok, C. Robert, W.-J. Hwu, J. S. Weber, A. Ribas, F. S. Hodi, A. M. Joshua, R. Kefford, P. Hersey, R. Joseph, T. C. Gangadhar, R. Dronca, A. Patnaik, H. Zarour, C. Roach, G. Toland, J. K. Lunceford, X. N. Li, K. Emancipator, M. Dolled-Filhart, S. P. Kang, S. Ebbinghaus, O. Hamid, Programmed death-ligand 1 expression and response to the anti-programmed death 1 antibody pembrolizumab in melanoma. *J. Clin. Oncol.* **34**, 4102–4109 (2016). [doi:10.1200/JCO.2016.67.2477](https://doi.org/10.1200/JCO.2016.67.2477) [Medline](#)